Anisotropic Metasurface for Realizing Cross Polarization Conversion based on a Symmetry Breaking Meta-Structures

Muhammad Ali[1], Talha Shahid Alvi[1]

[1]Department of Electrical Engineering, Information Technology University, Lahore, Pakistan

Abstract

In this research, we present the reflective cross-polarization conversion metasurface operating in the X- and Ku band of microwave frequencies. The proposed polarization converting device comprises a cross-shaped meta-structure surrounded with a split ring resonator. We have numerically calculated and showed that the proposed metasurface manifests 90% PCR in the operating band from 8.5-16 GHz. It is noticed that the outer split ring resonator is the main contributor in enhancing the cross-component of the reflected wave, which rotates the incident wave into its orthogonal counterpart. Furthermore, it can also be scalable to other operating bands by carefully selecting the materials and optimizing the design parameters. This kind of reflective meta-device would be prudent for the applications of beam reflectors, antennas, and holography.

Keywords

metasurface, microwave frequency, polarization conversion, symmetry breaking

I. Introduction

After the primary effort by Landy et. al. in 2008 [1] on single and narrow-band Gigahertz (GHz) perfect absorber, an enormous emphasis awakened of the optics and photonics researchers towards this stimulating area [2-10]. Thereafter, a variety of metasurface based EM and optical components has been realized including single, dual, triple, multi-band, wide-band, single- and multi- layer etc. ranging from the microwave-infrared range [11-16]. In addition to meta-absorbers, polarization converters had also gained huge significance owning to their many applications in antennas, holograms, transmissive surfaces, beam splitters, wireless communication and imaging etc. [17-25].

Previously, polarization conversion phenomena can be obtained by using the conventional approaches of optical grating, dichroic crystals and birefringence effect etc. [26-29] These methods limit the practicality in real applications due to the bulky weight, narrow bandwidth and costly fabrication process [30-37]. In recent years, a new class of two dimensional (2D) surfaces also called metasurfaces have been broadly employed to model various microwave and optical components including sensors, antennas, waveguides, absorbers and polarization converters etc. [33, 38-43] These 2D planar surfaces are composed of man-made artificially fashioned meta-molecules possesses different rotation, shapes, size and materials etc. Through these metasurfaces, electromagnetic (EM) waves can be manipulated by altering their periodic elements and design parameters to achieve exotic and unusual features which cannot be realized with natural materials [5, 15, 44].

Polarization conversion metasurfaces can be modeled in two different operation modes, reflection mode and transmission mode [8]. In reflection mode, anisotropic resonators play a role to control the EM reflection of the incident waves and to rotate into its orthogonal component [45-48]. A lot of research has also been conducted in anisotropic reflective metasurfaces to attain cross- and circular polarization conversion. In transmission mode, chiral structures are used to alter the transmission of incoming EM waves and to use them in achieving the polarization transformation. Similarly, people also implemented chiral metasurfaces in different configuration including single- and multi- layer etc. [49-52]. Most of the implemented devices rely on multi-layer and multi-faceted arrangements [53-55]. Advanced and modern communication systems demand highly efficient, broadband and single-layer polarization conversion metasurface.

In this paper, authors' motive to investigate highly efficient wideband metasurface which can transform the linearly polarized EM waves into its counter orthogonal component. Our reported meta-device converts the linearly polarized waves into its cross component over a broad spectrum of 8.5 to 16 GHz. The proposed metasurface operates in the reflection mode having efficiency of more than 90%. The designed configuration possesses three-layer scheme, i.e., top anisotropic metasurface, middle lossy dielectric spacer and bottom ground film. Furthermore, the proposed architecture can also be scalable to mm-wave and terahertz band. This kind of reflective meta-device would be prudent for the applications of antennas, imaging and beam generations.

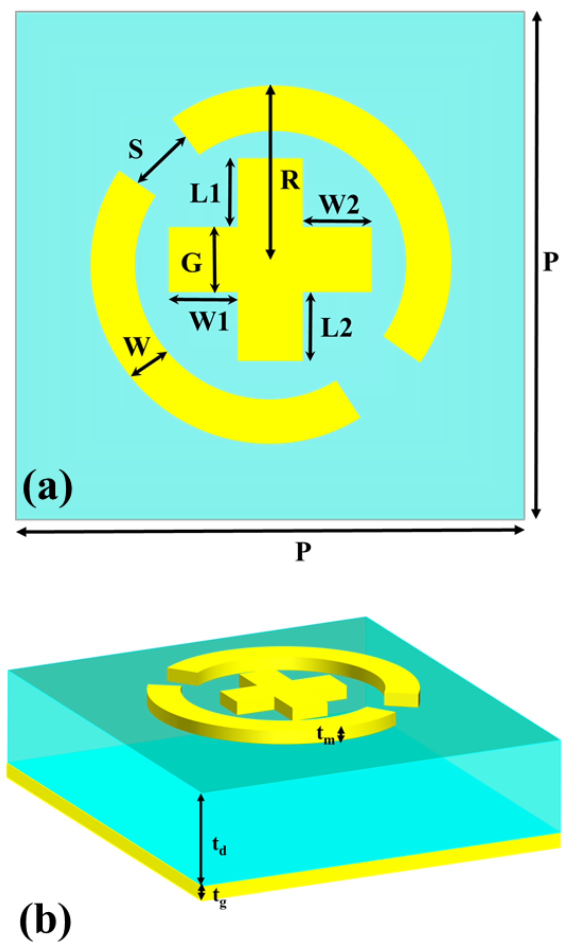

Fig. 1. Schematic of the proposed symmetry breaking metasurface along with its geometric characteristics, where P = 8 mm, R = 3.14 mm, W = 0.9 mm, G = 0.8 mm, W1 = W2 = 1.6 mm, L1 = 1.7 mm, L2 = 1.5 mm, S = 0.25 mm, td = 2 mm and tm = tg = 0.035 mm (a) front view and (b) prospective view

II. Design Technique

The meta-unit cell is composed of a + sign shaped patch antenna surrounded with a circular split-ring resonator. The design procedure, modeling and simulation are carried out by employing the frequency-domain EM tool CST studio [56-57]. To export its electromagnetic features, as shown in Fig. 1. The proposed meta-design is analyzed by considering the easily available EM solver, CST-Studio, which uses unit-cell boundary excitations across the *x-y* direction and open along the *z*-axis. The linearly x-polarized electromagnetic wave (EM) is taken as an input source to excite the symmetry breaking polarizing metasurface. The reflected co- component along with cross-polarized reflection parameter are computed and depicted in Fig. 2. It has been observed in Fig. 2 that the cross-polarized parameter is approaching its maximum value for the operating frequency from 8.5 GHz to 16 GHz, whereas the co-polarized reflection component attains its minimum value (ref. Fig. 2).

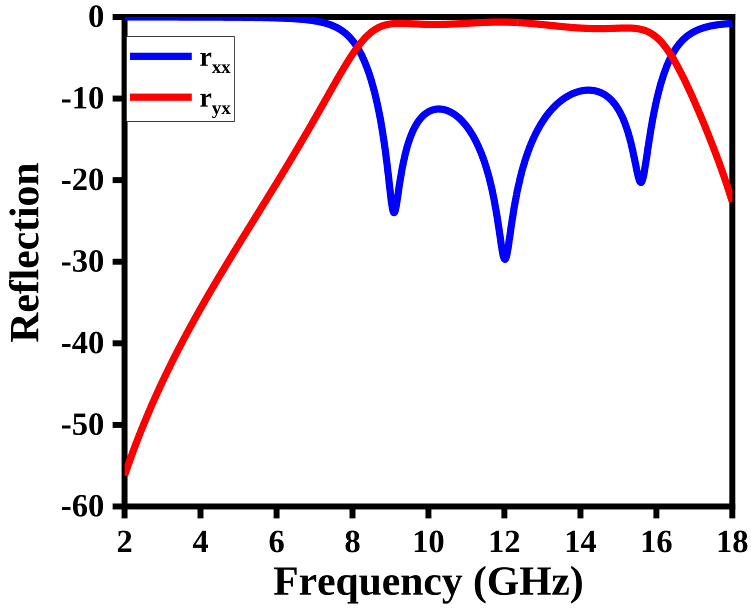

Fig.2. Simulated reflection features of the proposed symmetry breaking metasurface

III. Result and Discussion

When an EM wave falls on the top surface of the metamaterial, its overall absorption is determined from the following equation [1].

$$A(\omega) = 1 - T(\omega) - R(\omega) \quad (1)$$

Where,

$T(\omega) = |t_{xx}(\omega)|^2 + |t_{yx}(\omega)|^2$ and $R(\omega) = |r_{xx}(\omega)|^2 + |r_{yx}(\omega)|^2$ are the transmitted and reflected energies of the designed metasurface. The subscript (*xx*) and (*yx*) depict the co- and cross components respectively. The transmitted energy demolishes due to the inclusion of thick metallic sheet at the bottom, so, the total absorption is mainly dependent on the reflection component of the proposed metasurface. The actual absorption of the designed metasurface is below 10% because the designed has a large cross-reflection component as depicted in Fig. 2. The actual absorption of the metasurface is below 10% from 8.5-16 GHz.

The capability to convert the EM waves into its cross-polarizing can be measured in terms of its polarization conversion ratio (PCR), stated as [8].

$$\mathrm{PCR} = \frac{|R_{yx}|^2}{|R_{yx}|^2 + |R_{xx}|^2} \qquad (2)$$

Figure 3 demonstrates the converting efficiency of the proposed symmetry breaking metasurface as more than 90% across the large operating band (8.5-16 GHz). Therefore, the proposed symmetry breaking anisotropic device can be treated as a broadband polarization converter rather than a meta-absorber. Further, we can predict that the anisotropic structures can give us the polarization conversion features and they are very suitable for the implementation of polarization conversion metasurfaces in advanced systems. As it has a very large cross-component of reflection, so it gives a very poor absorption results.

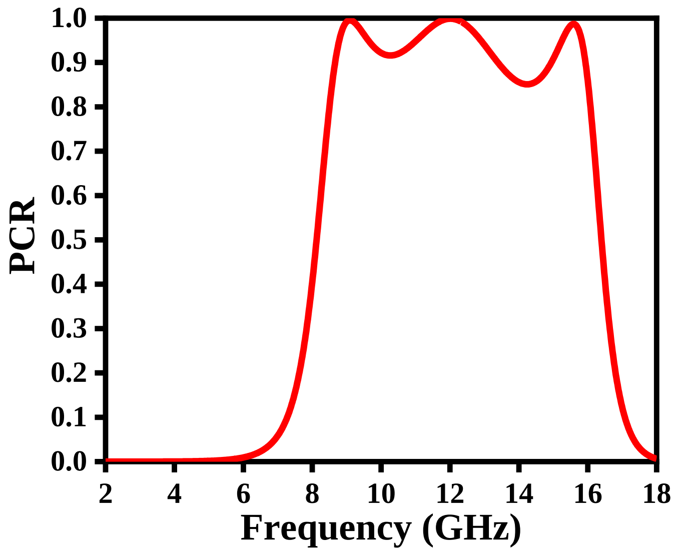

Fig. 3. Simulated conversion efficiency of the proposed symmetry breaking metasurface.

To justify the performance of the discussed polarization converter, the u- and v- polarized components and their phase difference are also plotted in Figure 4. For a linear cross-polarization converter, $r_{uu} = r_{vv} = 1$, and $\Delta\phi = \pm n\pi$, n being an integer. It is obvious from Figure 4(b) that the magnitude of r_{uu} and r_{vv} are close to 1, but at some points it decreases due to the Ohmic losses. It is also shown in Figure 4(c) that the phase difference is also close to −180 and 180 for the operating band from 8.5-16 GHz.

In this section, we verify the reflective cross-polarization conversion metasurface working in the X and Ku band of microwave frequencies spectrum. We have numerically designed and revealed that the proposed metasurface displays 90% PCR in the operating microwave frequencies from 8.5-16 GHz. Furthermore, its geometry can also be ascendable to other operating frequencies band by carefully picking the materials and adjusting the design parameters. This kind of reflective meta-device would be prudent for the applications of beam reflectors, antennas, and holography.

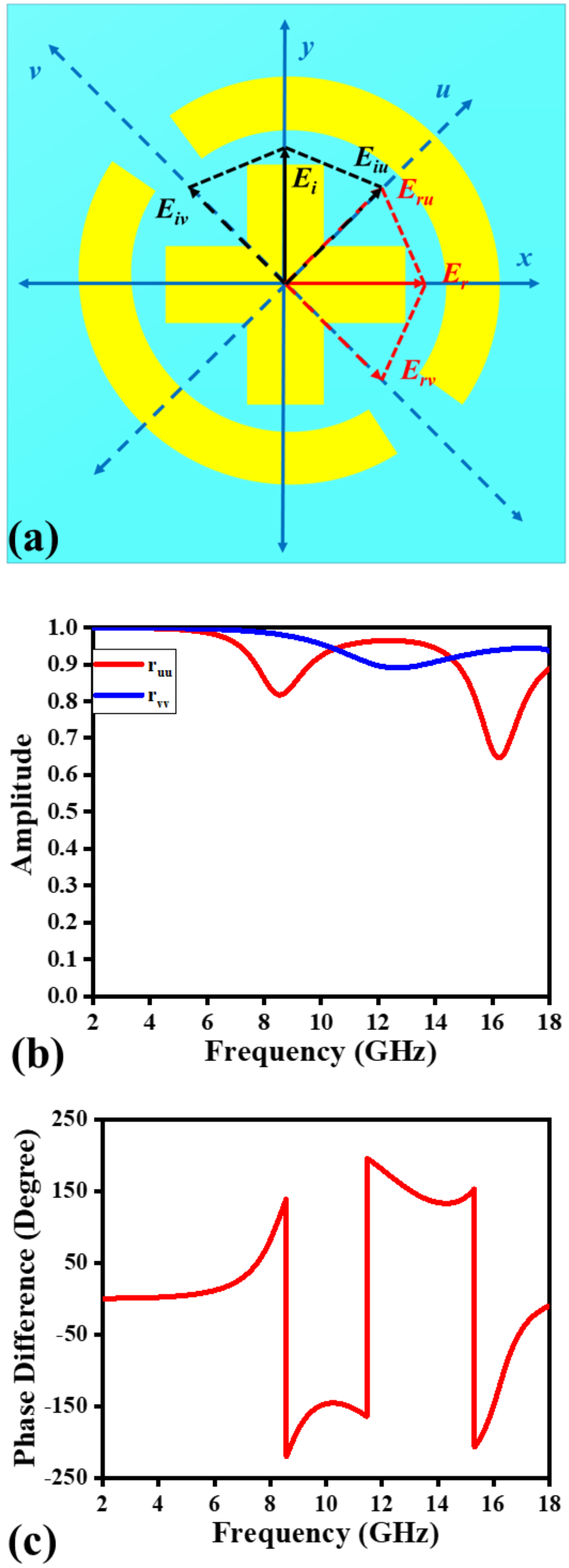

Fig. 4. Realization of the unit vectors of the proposed symmetry breaking metasurface along u- and v- axis as shown in the diagram, (a) depiction of the input (incident) and output (reflected) of the EM waves along u- v axis (b) spectra of amplitude and (c) phase difference representation.

IV. CONCLUSION

In summary, a highly efficient wideband linear reflective polarization rotator was investigated in this study. This meta-device possesses three-layer device configuration, top and bottom metallic layers and middle lossy dielectric spacer. The PCM illustrated more than 90% efficiency over a broad spectral range ranging from 8.5-16 GHz. Moreover, the proposed reflective meta-device can also be extended for other operating regimes, i.e., THz and IR, if we carefully chose the constitutive materials and geometric parameters.

REFERENCES

[1] N. I. Landy, S. Sajuyigbe, J. J. Mock, D. R. Smith, and W. J. Padilla, "Perfect metamaterial absorber," *Physical review letters,* vol. 100, no. 20, p. 207402, 2008.

[2] A. Hosseini and Y. Massoud, "A low-loss metal-insulator-metal plasmonic bragg reflector," *Optics express,* vol. 14, no. 23, pp. 11318-11323, 2006.

[3] Y. Zhao, M. Belkin, and A. Alù, "Twisted optical metamaterials for planarized ultrathin broadband circular polarizers," *Nature communications,* vol. 3, no. 1, pp. 1-7, 2012.

[4] A. Hosseini and Y. Massoud, "Nanoscale surface plasmon based resonator using rectangular geometry," *Applied Physics Letters,* vol. 90, no. 18, p. 181102, 2007.

[5] N. Yu and F. Capasso, "Flat optics with designer metasurfaces," *Nature materials,* vol. 13, no. 2, pp. 139-150, 2014.

[6] J. Laska *et al.*, "Random sampling for analog-to-information conversion of wideband signals," in *2006 IEEE Dallas/CAS Workshop on Design, Applications, Integration and Software*, 2006: IEEE, pp. 119-122.

[7] A. Nieuwoudt and Y. Massoud, "Evaluating the impact of resistance in carbon nanotube bundles for VLSI interconnect using diameter-dependent modeling techniques," *IEEE Transactions on Electron Devices,* vol. 53, no. 10, pp. 2460-2466, 2006.

[8] H. Zhu, S. Cheung, K. L. Chung, and T. I. Yuk, "Linear-to-circular polarization conversion using metasurface," *IEEE transactions on antennas and propagation,* vol. 61, no. 9, pp. 4615-4623, 2013.

[9] S. Kirolos, T. Ragheb, J. Laska, M. F. Duarte, Y. Massoud, and R. G. Baraniuk, "Practical issues in implementing analog-to-information converters," in *2006 6th International Workshop on System on Chip for Real Time Applications*, 2006: IEEE, pp. 141-146.

[10] A. Nieuwoudt and Y. Massoud, "Understanding the impact of inductance in carbon nanotube bundles for VLSI interconnect using scalable modeling techniques," *IEEE Transactions on Nanotechnology,* vol. 5, no. 6, pp. 758-765, 2006.

[11] T. Ragheb, J. N. Laska, H. Nejati, S. Kirolos, R. G. Baraniuk, and Y. Massoud, "A prototype hardware for random demodulation based compressive analog-to-digital conversion," in *2008 51st Midwest Symposium on Circuits and Systems*, 2008: IEEE, pp. 37-40.

[12] Kirolos, Sami, and Yehia Massoud. "Adaptive SRAM design for dynamic voltage scaling VLSI systems." In 2007 50th Midwest Symposium on Circuits and Systems, pp. 1297-1300. IEEE, 2007.

[13] A. Hosseini, H. Nejati, and Y. Massoud, "Modeling and design methodology for metal-insulator-metal plasmonic Bragg reflectors," *Optics express,* vol. 16, no. 3, pp. 1475-1480, 2008.

[14] A. Nieuwoudt and Y. Massoud, "On the optimal design, performance, and reliability of future carbon nanotube-based interconnect solutions," *IEEE transactions on electron devices,* vol. 55, no. 8, pp. 2097-2110, 2008.

[15] Ragheb, Tamer, Arthur Nieuwoudt, and Yehia Massoud. "Modeling of 3.1-10.6 GHz CMOS filter-based low noise amplifier for ultra-wideband receivers." In 2006 IEEE Annual Wireless and Microwave Technology Conference, pp. 1-5. IEEE, 2006.

[16] Y. Massoud, S. Majors, T. Bustami, and J. White, "Layout techniques for minimizing on-chip interconnect self inductance," in *Proceedings of the 35th annual Design Automation Conference*, 1998, pp. 566-571.

[17] Y. Massoud and J. White, "Simulation and modeling of the effect of substrate conductivity on coupling inductance and circuit crosstalk," *IEEE Transactions on Very Large Scale Integration (VLSI) Systems,* vol. 10, no. 3, pp. 286-291, 2002.

[18] M. Mondal *et al.*, "Thermally robust clocking schemes for 3D integrated circuits," in *2007 Design, Automation & Test in Europe Conference & Exhibition*, 2007: IEEE, pp. 1-6.

[19] T. Ragheb *et al.*, "Implementation models for analog-to-information conversion via random sampling," in *2007 50th Midwest Symposium on Circuits and Systems*, 2007: IEEE, pp. 325-328.

[20] X. Yin, Z. Ye, J. Rho, Y. Wang, and X. Zhang, "Photonic spin Hall effect at metasurfaces," *Science,* vol. 339, no. 6126, pp. 1405-1407, 2013.

[21] Y. Massoud and A. Nieuwoudt, "Modeling and design challenges and solutions for carbon nanotube-based interconnect in future high performance integrated circuits," *ACM Journal on Emerging Technologies in Computing Systems (JETC),* vol. 2, no. 3, pp. 155-196, 2006.

[22] A. Nieuwoudt and Y. Massoud, "On the impact of process variations for carbon nanotube bundles for VLSI interconnect," *IEEE Transactions on Electron Devices,* vol. 54, no. 3, pp. 446-455, 2007.

[23] C. Hu, X. Li, Q. Feng, X. N. Chen, and X. Luo, "Investigation on the role of the dielectric loss in metamaterial absorber," *Optics Express,* vol. 18, no. 7, pp. 6598-6603, 2010.

[24] Y. Massoud, S. Majors, J. Kawa, T. Bustami, D. MacMillen, and J. White, "Managing on-chip inductive effects," *IEEE Transactions on Very Large Scale Integration (VLSI) Systems,* vol. 10, no. 6, pp. 789-798, 2002.

[25] Y. Massoud, J. Kawa, D. MacMillen, and J. White, "Modeling and analysis of differential signaling for minimizing inductive cross-talk," in *Proceedings of the 38th annual Design Automation Conference*, 2001, pp. 804-809.

[26] A. Nieuwoudt and Y. Massoud, "Variability-aware multilevel integrated spiral inductor synthesis," *IEEE Transactions on Computer-Aided Design of Integrated Circuits and Systems,* vol. 25, no. 12, pp. 2613-2625, 2006.

[27] A. Hosseini, T. Ragheb, and Y. Massoud, "A fault-aware dynamic routing algorithm for on-chip networks," in *2008 IEEE International Symposium on Circuits and Systems*, 2008: IEEE, pp. 2653-2656.

[28] M. Neviere, R. Petit, and M. Cadilhac, "About the theory of optical grating coupler-waveguide systems," *Optics Communications,* vol. 8, no. 2, pp. 113-117, 1973.

[29] A. Nieuwoudt and Y. Massoud, "Multi-level approach for integrated spiral inductor optimization," in *Proceedings of the 42nd annual Design Automation Conference*, 2005, pp. 648-651.

[30] Y. I. Ismail and E. G. Friedman, *On-chip inductance in high speed integrated circuits*. Springer Science & Business Media, 2001.

[31] Y. Massoud and J. White, "Improving the generality of the fictitious magnetic charge approach to computing inductances in the presence of permeable materials," in *Proceedings of the 39th annual Design Automation Conference*, 2002, pp. 552-555.

[32] Y. Cai and K. D. Xu, "Tunable broadband terahertz absorber based on multilayer graphene-sandwiched plasmonic structure," *Opt Express*, vol. 26, no. 24, pp. 31693-31705, Nov 26 2018, doi: 10.1364/OE.26.031693.

[33] A. Nieuwoudt, T. Ragheb, and Y. Massoud, "SOC-NLNA: Synthesis and optimization for fully integrated narrow-band CMOS low noise amplifiers," in *2006 43rd ACM/IEEE Design Automation Conference*, 2006: IEEE, pp. 879-884.

[34] S. Eachempati, A. Nieuwoudt, A. Gayasen, N. Vijaykrishnan, and Y. Massoud, "Assessing carbon nanotube bundle interconnect for future FPGA architectures," in *2007 Design, Automation & Test in Europe Conference & Exhibition*, 2007: IEEE, pp. 1-6.

[35] Y. Massoud, M. Alam, and A. Nieuwoudt, "On the selection of spectral zeros for generating passive reduced order models," in *2006 6th International Workshop on System on Chip for Real Time Applications*, 2006: IEEE, pp. 160-164.

[36] A. Nieuwoudt and Y. Massoud, "Predicting the performance of low-loss on-chip inductors realized using carbon nanotube bundles," *IEEE Transactions on Electron Devices,* vol. 55, no. 1, pp. 298-312, 2007.

[37] J. Saikawa, M. Miyazaki, M. Fujii, H. Ishizuki, and T. Taira, "High-energy, broadly tunable, narrow-bandwidth mid-infrared optical parametric system pumped by quasi-phase-matched devices," *Optics letters,* vol. 33, no. 15, pp. 1699-1701, 2008.

[38] Y. Massoud and J. White, "FastMag: a 3-D magnetostatic inductance extraction program for structures with permeable materials," in *Proceedings of the 2002 IEEE/ACM international conference on Computer-aided design*, 2002, pp. 478-484.

[39] A. Nieuwoudt, T. Ragheb, H. Nejati, and Y. Massoud, "Numerical design optimization methodology for wideband and multi-band inductively degenerated cascode CMOS low noise amplifiers," *IEEE Transactions on Circuits and Systems I: Regular Papers,* vol. 56, no. 6, pp. 1088-1101, 2008.

[40] M. Mondal and Y. Massoud, "Reducing pessimism in RLC delay estimation using an accurate analytical frequency dependent model for inductance," in *ICCAD-2005. IEEE/ACM International Conference on Computer-Aided Design, 2005.*, 2005: IEEE, pp. 691-696.

[41] S. Kirolos, Y. Massoud, and Y. Ismail, "Power-supply-variation-aware timing analysis of synchronous systems," in *2008 IEEE International Symposium on Circuits and Systems*, 2008: IEEE, pp. 2418-2421.

[42] S. Eachempati, N. Vijaykrishnan, A. Nieuwoudt, and Y. Massoud, "Predicting the performance and reliability of future field programmable gate arrays routing architectures with carbon nanotube bundle interconnect," *IET circuits, devices & systems,* vol. 3, no. 2, pp. 64-75, 2009.

[43] A. Nieuwoudt, M. S. McCorquodale, R. T. Borno, and Y. Massoud, "Efficient analytical modeling techniques for rapid integrated spiral inductor prototyping," in *Proceedings of the IEEE 2005 Custom Integrated Circuits Conference, 2005.*, 2005: IEEE, pp. 281-284.

[44] Mondal, Mosin, Andrew Ricketts, Sami Kirolos, Tamer Ragheb, Greg Link, Vijaykrishnan Narayanan, and Yehia Massoud. "Mitigating thermal effects on clock skew with dynamically adaptive drivers." In 8th International Symposium on Quality Electronic Design (ISQED'07), pp. 67-72. IEEE, 2007.

[45] H. Chen *et al.*, "Ultra-wideband polarization conversion metasurfaces based on multiple plasmon resonances," *Journal of Applied Physics,* vol. 115, no. 15, p. 154504, 2014.

[46] Pfetsch, Stephen, Tamer Ragheb, Jason Laska, Hamid Nejati, Anna Gilbert, Martin Strauss, Richard Baraniuk, and Yehia Massoud. "On the feasibility of hardware implementation of sub-Nyquist random-sampling based analog-to-information conversion." In 2008 IEEE International Symposium on Circuits and Systems, pp. 1480-1483. IEEE, 2008.

[47] A. Nieuwoudt and Y. Massoud, "Analytical wide-band modeling of high frequency resistance in integrated spiral inductors," *Analog Integrated Circuits and Signal Processing,* vol. 50, no. 2, pp. 133-136, 2007.

[48] M. Mondal, T. Ragheb, X. Wu, A. Aziz, and Y. Massoud, "Provisioning on-chip networks under buffered rc interconnect delay variations," in *8th International Symposium on Quality Electronic Design (ISQED'07)*, 2007: IEEE, pp. 873-878.

[49] T. Ragheb and Y. Massoud, "On the modeling of resistance in graphene nanoribbon (GNR) for future interconnect applications," in *2008 IEEE/ACM International Conference on Computer-Aided Design*, 2008: IEEE, pp. 593-597.

[50] A. Nieuwoudt, T. Ragheb, and Y. Massoud, "Hierarchical optimization methodology for wideband low noise amplifiers," in *2007 Asia and South Pacific design automation conference*, 2007: IEEE, pp. 68-73.

[51] P. Fei *et al.*, "Versatile Cross-Polarization Conversion Chiral Metasurface for Linear and Circular Polarizations," *Advanced Optical Materials,* vol. 8, no. 13, p. 2000194, 2020.

[52] A. Nieuwoudt, T. Ragheb, H. Nejati, and Y. Massoud, "Increasing manufacturing yield for wideband RF CMOS LNAs in the presence of process variations," in *8th International Symposium on Quality Electronic Design (ISQED'07)*, 2007: IEEE, pp. 801-806.

[53] A. Nieuwoudt and Y. Massoud, "Robust automated synthesis methodology for integrated spiral inductors with variability," in *ICCAD-2005. IEEE/ACM International Conference on Computer-Aided Design, 2005.*, 2005: IEEE, pp. 502-507.

[54] Y. Yang *et al.*, "Graphene-based multilayered metamaterials with phototunable architecture for on-chip photonic devices," *Acs Photonics,* vol. 6, no. 4, pp. 1033-1040, 2019.

[55] A. Nieuwoudt, M. S. McCorquodale, R. T. Borno, and Y. Massoud, "Accurate analytical spiral inductor modeling techniques for efficient design space exploration," *IEEE Electron Device Letters,* vol. 27, no. 12, pp. 998-1001, 2006.

[56] Gao, Liang S., Fuhai Li, Yaliang Yang, Jiong Xing, Ahmad A. Hammoudi, Hong Zhao, Yubo Fan et al. "On-the-spot lung cancer differential diagnosis by label-free, molecular vibrational imaging and knowledge-based classification." Journal of biomedical optics 16, no. 9 (2011): 096004.

[57] Song, Yi-Chuan, Jun Ding, Chen-Jiang Guo, Yu-Hui Ren, and Jia-Kai Zhang. "Ultra-broadband backscatter radar cross section reduction based on polarization-insensitive metasurface." IEEE Antennas and Wireless Propagation Letters 15 (2015): 329-331.